Two-photon absorption spectroscopy of rubrene single crystals

Pavel Irkhin and Ivan Biaggio

Department of Physics, Lehigh University, Bethlehem, Pennsylvania 18015, USA

We determine the wavelength dependence of the two-photon absorption cross section in rubrene single crystals both by direct measurement of nonlinear transmission and from the two-photon excitation spectrum of the photoluminescence. The peak two-photon absorption coefficient for *b*-polarized light was found to be $(4.6 \pm 1) \times 10^{-11}$ m/W at a wavelength of 850 ± 10 nm. It is 2.3 times larger for *c*-polarized light. The lowest energy two-photon excitation peak corresponds to an excited state energy of 2.92 ± 0.04 eV and it is followed by a vibronic progression of higher energy peaks separated by ~ 0.14 eV.

Two-photon absorption (TPA) in centrosymmetric materials and molecules can provide information on excited states that cannot otherwise be accessed by one-photon transitions, and it can be an important complement to conventional absorption or photoluminescence (PL) spectroscopy. Here we use TPA to complete our recent study [1] of absorption and PL spectroscopy in the organic molecular crystal rubrene.

Among several organic materials that have been studied as organic semiconductors, and used, e.g., in organic field-effect transistors [2–4], photovoltaic cells [5], or light emitting diodes [6], rubrene (5,6,11,12-tetraphenylnaphthacene) single crystals are of particular interest because of several compelling properties, including one of the highest room-temperature charge carrier mobilities in an organic material (~ 10 cm^2 V^{-1} s^{-1} for holes in field-effect transistors [2,7–9]), high photoconductivity [10–13], and a large triplet exciton diffusion length [14].

Rubrene belongs to the group of polycyclic aromatic hydrocarbons and consists of a molecule with a backbone structurally equal to tetracene [Fig. 1(a)] with four substituted phenyl groups attached to the two internal rings. This molecule as it is found in rubrene single crystals [15] is centrosymmetric, with a symmetry corresponding to the point group $2/m$, or C_{2h}, and a twofold axis of rotation (M axis) along the short backbone. This molecular structure and the direction of the L, N, and M axes are shown in Fig. 1(a). Vapor transport grown rubrene crystals are orthorhombic [15], with D_{2h}^{18} (or mmm) point group and four molecules per unit cell. In this Rapid Communication, as in Ref. [1], we define the crystallographic axes in the space group *Acam*, in which the lattice constants are $a = 14.4$ Å, $b = 7.18$ Å, and $c = 26.9$ Å, consistent with the labeling of the axes used in previous transport studies [8,10,14]. The high hole and exciton mobility values in rubrene crystals are found along the b axis, which is the crystallographic direction characterized by a herringbone molecular packing with an efficient π overlap. Figure 1(b) shows the molecular stacking in the ab plane of the crystal. The L and N axes of the molecules are parallel to the ab plane of the crystal, while the M axis of all molecules is oriented along the c direction.

Two-photon absorption (TPA) in rubrene leads both to the expected intensity-dependent attenuation of the incident light and to photoluminescence (PL). In this work we used both physical effects to characterize the magnitude as well as the wavelength dependence of TPA. We first describe a measurement of the nonlinear transmittivity and two-photon induced PL power for varying excitation pulse intensity at a wavelength of 840 nm. Then, we present the results of several similar measurements that were performed at different wavelengths in the range between 720 and 900 nm, and of a separate determination of two-photon induced PL power versus wavelength, which we combine with the more complete power dependence measured at 840 nm to extract the full dispersion and magnitude of TPA in rubrene. Finally, we discuss the dependence of two-photon induced PL power from the polarization of the excitation light.

The intensity-dependent, nonlinear attenuation of light intensity with propagation distance z can be described as

$$\frac{dI(z)}{dz} = -\alpha I(z) - \beta [I(z)]^2, \tag{1}$$

where I is the light intensity, α is the absorption constant, and $\beta = N\sigma$ is the TPA coefficient, where N is the number density of active molecules with average TPA cross section σ. For a collimated laser beam with a Gaussian spatial and temporal profile (beam waist w_0, pulse duration τ) the intensity depends on the distance r from the beam axis and the time t as

$$I(r,t) = I_0 e^{-2r^2/w_0^2 - t^2/\tau^2}, \tag{2}$$

where the peak intensity I_0 is related to the total pulse energy $E_p(0)$ by

$$I_0 = \frac{2}{\pi^{3/2} w_0^2 \tau} E_p(0). \tag{3}$$

In the presence of nonlinear absorption the total pulse energy in a collimated beam with constant diameter depends on the propagation distance z as [16]

$$E_p(z) = \int_{-\infty}^{\infty} \int_{0}^{\infty} 2\pi r \frac{I(r,t)}{1 + \beta I(r,t)z} dr\, dt \tag{4}$$

$$= \frac{\pi w_0^2}{2\beta z} \int_{-\infty}^{\infty} \ln[1 + \beta I_0 z e^{-t^2/\tau^2}] dt, \tag{5}$$

from which one can derive a nonlinear transmittivity $T_{\text{NL}} = E_p(z)/E_p(0)$:

$$T_{\text{NL}} = \frac{1}{\sqrt{\pi} \beta I_0 z \tau} \int_{-\infty}^{\infty} \ln[1 + \beta I_0 z e^{-t^2/\tau^2}] dt. \tag{6}$$
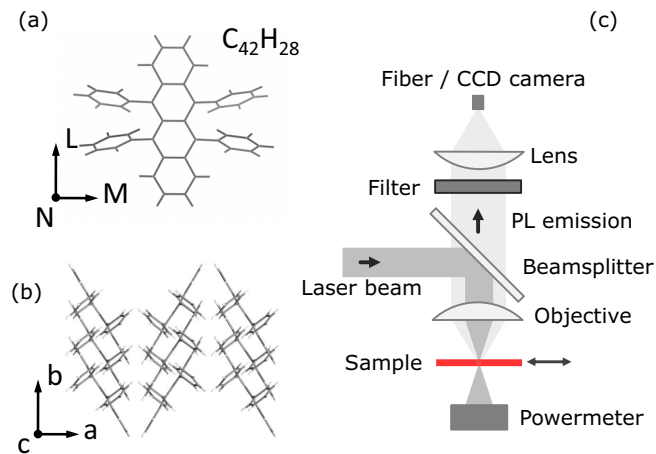
FIG. 1. (Color online) (a) Rubrene molecule. (b) Rubrene crystal structure in the *ab* plane. (c) Scheme of the experimental setup for TPA; the photoluminescence is imaged either on a fiber or on an image sensor (CCD) used to control the good surface quality of the sample.
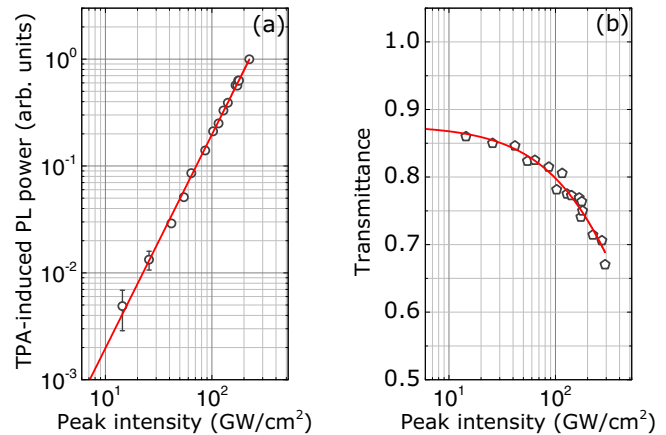

FIG. 2. (Color online) (a) Excitation intensity dependence of the TPA-induced fluorescence power (the solid curve is a quadratic dependence). (b) Transmission of the crystal as a function of the peak excitation intensity [the solid curve is a fit obtained with Eq. (7)]. The incident light had a wavelength of 840 nm and was *b* polarized.

The above expression can be well approximated by [16]

$$T_{\text{NL}}^{\text{cw}} = \frac{1}{\beta I_0^{\text{cw}} z} \ln \left[1 + \beta I_0^{\text{cw}} z \right], \quad (7)$$

which would be valid for a continuous wave (cw) collimated Gaussian beam with peak intensity I_0^{cw}, if one defines $I_0^{\text{cw}} = 0.7 I_0$, with I_0 as given in Eq. (3). We find that this approximation follows the prediction of Eq. (6) at low intensities and delivers a result too small by only ∼5% at an attenuation $T_{\text{NL}} = 0.5$.

All measurements were performed with wavelength-tunable 1 ps laser pulses at a 1 kHz repetition rate, which were obtained from a Light Conversion traveling wave optical parametric amplifier system (TOPAS) pumped by a Clark-MXR CPA 2101 laser system. Crystal thicknesses were determined interferometrically and confirmed by direct optical imaging. The laser radiation was focused on the surface of rubrene crystals by a 10× microscope objective [Fig. 1(c)]. In this configuration, the Rayleigh length of the laser beam (∼100 μm) was much larger than the crystal thicknesses we used, providing a nearly constant beam diameter inside the samples. Since the two-photon excitation extends deep inside the sample, the emitted PL is subject to significant wavelength-dependent absorption, which severely impacts the shape of the PL spectrum [1]. But we confirmed, using a 2 μm thick crystal under 772 nm excitation, that the emitted TPA-induced PL spectrum matches, after correction for reabsorption, the intrinsic rubrene emission spectrum determined under one-photon excitation [1]. This remains true for all light polarizations and all excitation wavelengths that we have investigated, and it shows that after two-photon excitation the system has—in addition to other possible relaxation mechanisms [17]—a finite probability to relax back (either directly or indirectly via, e.g., singlet fission [17] followed at higher excitation densities by triplet fusion [13]) to the same singlet excited state reached after single-photon excitation.

We measured the nonlinear transmittivity and the induced PL power as a function of the excitation pulse intensity at 840 nm in a 13.5 μm thick rubrene crystal. The excitation light was incident perpendicular to the *ab* surface of the sample and was polarized along the *b* axis. The beam waist in the crystal was $w_0 = 5.1$ μm, directly obtained from an image of the beam cross section. The pulse duration was given by $\tau = 0.43$ ps [see Eq. (2)], as determined by an autocorrelation experiment. The peak intensity I_0 was calculated from the measured pulse energies using Eq. (3), which gave $I_0 = 64$ GW/cm^2 for a pulse energy of 20 nJ. The results for the PL power versus excitation intensity, shown in Fig. 2(a), confirm the expected quadratic dependence that is typical of TPA. The transmission of the sample, in the same range of excitation pulse intensities, is shown in Fig. 2(b). At low pulse intensities it is determined by reflection losses of 0.064 at the two surfaces of the crystal, corresponding to a refractive index of ∼1.68 for *b*-polarized light. At higher pulse energies the transmission decreases, and the data can be fitted very well using Eq. (7) with $I_0^{\text{cw}} = 0.7 I_0$ and only β as a fitting parameter. From this one-parameter fit of the data in Fig. 2(b) we obtain a TPA coefficient of $\beta_b(840 \text{ nm}) = (2.3 \pm 0.5) \times 10^{-11}$ m/W.

We used the same rubrene sample to study the wavelength dependence of TPA in the interval between 750 and 920 nm by taking measurements every 10 nm. Both nonlinear transmission and PL power were determined following the procedure described above. At each wavelength, we first observed the sample surface under the microscope to confirm that it was high quality and free of defects. Next, the *b*-polarized excitation light was focused on the same spot, and the sample transmission was measured by translating it in and out of the laser beam. This was first done at low excitation intensities, and then the measurement was repeated at higher excitation intensities where significant TPA occurred, while at the same time measuring the emitted PL power. At each measurement wavelength, the TPA coefficient β_b was obtained from the two measurements of sample transmission using Eq. (7). This procedure is faster, but less precise, than the full measurement
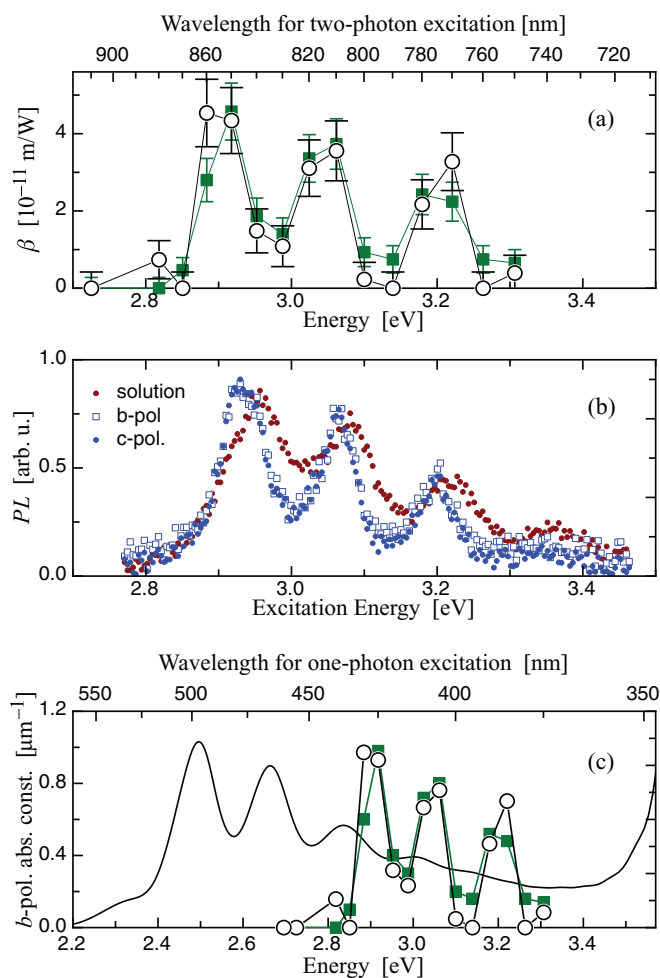
FIG. 3. (Color online) Spectral dependence of theTPA coefficient for b-polarized excitation in rubrene single crystals. (a) Direct measurement of the TPA coefficient (open circles) compared with the results of two-photon induced PL (solid squares, scaled to match the magnitude of the TPA coefficient). (b) Wavelength scan, obtained in a different experiment, comparing two-photon induced PL in a rubrene solution and in a rubrene crystal for b and c polarization (the two spectra are normalized). (c) b-polarized linear absorption (solid curve) compared to TPA spectrum [circles and squares, repeated from (a)]. The bottom horizontal axes in all plots give the excitation energy, equal to twice the photon energy for TPA.

at 840 nm that we presented above. The higher precision of the latter was taken into account by rescaling the data obtained during the wavelength scan to match the TPA coefficient value obtained earlier at 840 nm (a correction of ~30%). Figure 3(a) shows the resulting data for the wavelength-dependent TPA coefficient. The data obtained from the detected PL power, scaled to match the TPA-coefficient data, are also included.

The wavelength dependences obtained from the nonlinear transmission measurement and from the variation in photoluminescence power match each other very well. The resulting TPA spectrum was also confirmed using another experimental setup in which we simply observed the power of the TPA-induced PL while the laser wavelength was continuously scanned between 700 and 900 nm. Unfortunately, in this setup

it was not possible to measure the illumination power at the position of the sample and we could not obtain absolute data, but the denser data points provide additional information on the shape of the TPA spectrum. The TPA spectra obtained in this way are shown in Fig. 3(b) for a rubrene solution and for b- and c-polarized excitation in a single crystal. There is no notable difference between the two polarized single crystal spectra, which match quite well the measurements shown in Fig. 3(a). The single crystal spectrum is slightly shifted to lower energies with respect to the solution spectrum, similar to what happens for linear absorption [1].

In general, the TPA spectrum has the same characteristic vibronic progression as the absorption spectrum, but the distance between the vibronic replicas, at 0.14 eV vs 0.17 eV, is slightly smaller than for single-photon absorption [1]. The lowest energy TPA peak is found at 850 ± 10 nm (2.92 ± 0.04 eV), implying that the excited state reached by TPA is ~2.9 eV above the ground state. The corresponding TPA coefficient is $\beta_b(850 \text{ nm}) = (4.6 \pm 1) \times 10^{-11}$ m/W. This value can be used to obtain a molecular TPA cross section σ from $\beta_b = N\sigma$, where $N = 1.434 \times 10^{27}$ m^{-3} is the number density of rubrene molecules in the crystal. One finds $\sigma = 3.21 \times 10^{-38}$ m^4/W. Multiplication by the photon energy finally gives a molecular TPA cross section of $(7.5 \pm 2) \times 10^{-57}$ m^4 s photon^{-1} $= 75 \pm 20$ GM. This cross section must be understood as a projection of the molecular TPA properties onto the direction specified by the b axis of the crystal. Below we will show that TPA is 2.3 times stronger for light polarized along the c axis of rubrene than for light polarized along the b axis, which implies $\beta_c(850 \text{ nm}) \sim 10^{-10}$ m/W and a molecular TPA cross section of 170 ± 40 GM for an optical electric field along the M axis of the rubrene molecule.

The molecular TPA cross sections we obtained compare well to the theoretical value predicted by Ref. [18] (185 GM) but are significantly smaller than a value of 1000 GM recently reported by Ma *et al.* [17]. This latter value is much larger than the theoretical value of Ref. [18] and also much larger than typical values for organic molecules of similar size as rubrene. As an example the "AF-50" compound, which has been developed for TPA, has a TPA cross section of 30 GM (see Ref. [19]), and even optimized larger molecules tend to remain below 1000 GM [20]. The discrepancy between our results and those of Ma *et al.* [17] is also directly seen in the TPA coefficient of 52×10^{-11} m/W at 740 nm reported in Ref. [17], which is an order of magnitude larger than the peak value we find for b-polarized light at 850 nm. But the difference between the two experiments is even larger if one considers that our spectroscopy results discussed above imply a weaker TPA at 740 nm than the peak value we determined. One possible explanation for the discrepancy could stem from the fact that Ref. [17] used open aperture Z scan with a femtosecond laser at a repetition rate of 80 MHz. Under those conditions any excited states with a lifetime larger than the time interval of 12.5 ns between the pulses—for rubrene, the average lifetime of the singlet state in solution is 15 ns, while in pristine single crystals the lifetime of triplet excitons is 100 μs [21]—could accumulate during the laser exposure and possibly end up contributing to the Z-scan signal, thus increasing the perceived TPA magnitude depending on the wavelength-dependent TPA from those excited states (such

an effect could be particularly important in single crystals because of the very large density of long-lived triplet excitons formed by the extremely efficient singlet fission [13,21]). There is another difference between our work and that of Ma *et al.* [17] that we mention for completeness: We investigated pristine rubrene samples characterized by a PL emission spectrum emitted from the *ab* surface that peaks near 605 nm [1], while the samples used in Ref. [17] had an anomalous photoluminescence emission spectrum peaking near 650 nm (see Ref. [17], Fig. 1). It is not yet clear what the origin is of this anomalous photoluminescence emission spectrum [1,22].

The TPA spectrum in Fig. 3 implies an excited state with even parity (same as the ground state) at an energy of 2.92 eV. This value is surprising because previous computational results for the excited state energies of rubrene crystals [17,18,23] did not predict a two-photon accessible state in this range of energy. However, Ref. [18] obtained the first two-photon accessible state at ∼4.15 eV and the first one-photon state at ∼2.83 eV, which needs to be multiplied by 0.8 to match the experimental value of 2.32 eV for the optical transition energy to the first one-photon state [1]. If one were to apply the same factor to the two-photon excitation energy, one would obtain ∼3.4 eV, which is closer to what we have seen. But further analysis will be needed to better understand the difference between computational results and the experiment.

To better investigate the nature of the two-photon state we studied the anisotropy of TPA by measuring the induced PL for light polarized along all three axes of a rubrene crystal. To do this, we used the same experimental setup described above to focus the excitation laser on the *ab* and the *bc* surfaces of a crystal, and we compared the two-photon induced PL as the excitation polarization was rotated in the *ab* or *bc* plane. For this experiment we used an illumination at 772 nm (corresponding to a two-photon excitation near $2\hbar\omega \approx 3.2$ eV). Both excitation and PL collection occurred along the normal to the sample surface. The excitation power was kept constant while the crystal was rotated under illumination with linearly polarized light. The excitation intensity was in the range where two-photon induced PL was clearly visible, but was kept low enough, so that TPA took place without appreciable attenuation in the crystal, guaranteeing that the excitation volume probed by the confocal detection remained constant irrespective of the excitation polarization. The emitted PL power induced by every excitation polarization, which was collected without filtering its polarization, was dominated by the *c*-polarized light when using a *bc* facet, and was predominantly *b* polarized for an *ab* facet. The ratio between polarization components in each case was the same as for one-photon excitation [1]. We confirmed that both the polarization of the emitted PL and its spectrum did not depend on the polarization of the excitation light, or on its wavelength.

The variation of the two-photon induced PL power with excitation polarization is depicted in the polar plot of Fig. 4. The two-photon induced PL power for excitation polarization along the three main axes directly gives a TPA coefficient for *c*-polarized light that is 2.3 times larger than for *b*-polarized light, which is in turn four times larger than the coefficient for *a*-polarized light. The strong TPA for *c*-polarized light can be directly translated into a molecular TPA cross section
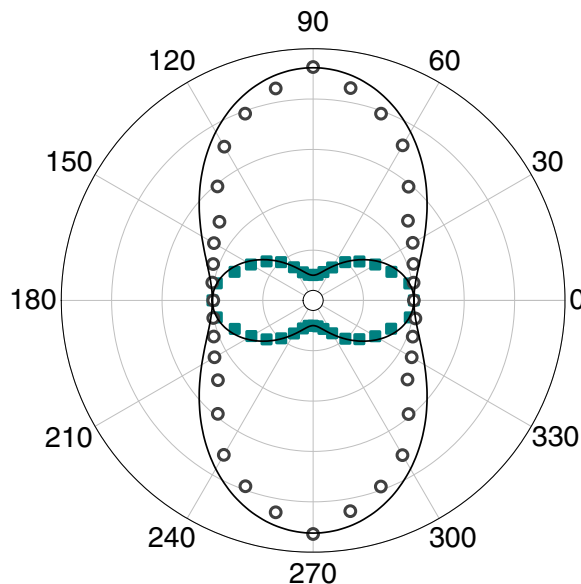

FIG. 4. (Color online) Polar plot of PL intensity vs the polarization of the excitation laser at 772 nm as it is varied in the *ab* (solid squares) and *bc* (open circles) planes of a rubrene crystal. The *b* axis of the crystal corresponds to an excitation angle of 0°. The *a* and *c* axes correspond to 90°. The solid curves are theoretical predictions (see text).

for optical field along the *M* axis of the rubrene molecule of ∼170 GM. In Fig. 4 the solid curves give the TPA predicted from the square of the projection on the incident optical electric field of a diagonal TPA tensor with elements in the ratio of 0.5:1:1.52 for light polarized along *a*, *b*, and *c*, respectively. For excitation polarization at an angle θ to the main axes with TPA coefficients β_1 and β_2, this angular dependence is of the form $(\sqrt{\beta_1}\cos^2\theta + \sqrt{\beta_2}\sin^2\theta)^2$. But we note that when the incident polarization is not parallel to a crystallographic axis, birefringence complicates the analysis, causing a propagation distance-dependent phase shift in the two optical field components that would influence the addition of the two corresponding probability amplitudes for TPA. Therefore, the solid curves in Fig. 4 are not expected to follow the data points for angles that do not correspond to the main axes. Despite this, the solid curve does closely follow the data for polarization in the *ab* plane, with small deviations only visible for the *bc*-plane data. This could be related to the combination of a smaller birefringence in the *ab* plane and the fact that our setup for this experiment was more efficient in collecting the PL emitted near the surface of the crystal.

In conclusion, we have experimentally determined the TPA spectrum of rubrene single crystals. The excitation spectrum is consistent with an excited state at an energy of 2.92 ± 0.04 eV above the ground state, and it is characterized by a vibronic progression similar to what is seen in linear absorption or emission spectra in rubrene single crystals [1]. The peak molecular TPA cross section of ∼170 GM at 850 nm is found for light polarized along the *M* axis of the molecule, corresponding to a *c*-polarized TPA coefficient in the crystal of $\beta_c(850\,\text{nm}) \sim 10^{-10}$ m/W, which is 2.3 times and 9.2 times stronger than for *b* and *a* polarization,

respectively. The emission spectrum obtained under TPA excitation deep inside the sample can be strongly affected by the anisotropic crystal absorption, but once corrected for these effects it has the same characteristics as the PL emission spectrum obtained under one-photon excitation, and it is independent from both excitation polarization and excitation wavelength.

[1] P. Irkhin, A. Ryasnyanskiy, M. Koehler, and I. Biaggio, Phys. Rev. B **86**, 085143 (2012).

[2] V. C. Sundar, J. Zaumseil, V. Podzorov, E. Menard, R. L. Willett, T. Someya, M. E. Gershenson, and J. A. Rogers, Science **303**, 1644 (2004).

[3] A. Briseno, R. Tseng, M.-M. Ling, E. Falcao, Y. Yang, F. Wudl, and Z. Bao, Adv. Mater. **18**, 2320 (2006).

[4] R. de Boer, M. Gershenson, A. Morpurgo, and V. Podzorov, Phys. Status Solidi A **201**, 1302 (2004).

[5] R. Tseng, R. Chan, V. Tung, and Y. Yang, Adv. Mater. **20**, 435 (2008).

[6] Y. Shao and Y. Yang, Appl. Phys. Lett. **86**, 073510 (2005).

[7] V. Podzorov, V. Pudalov, and M. Gershenson, Appl. Phys. Lett. **82**, 1739 (2003).

[8] V. Podzorov, E. Menard, A. Borissov, V. Kiryukhin, J. A. Rogers, and M. E. Gershenson, Phys. Rev. Lett. **93**, 086602 (2004).

[9] V. Podzorov and M. E. Gershenson, Phys. Rev. Lett. **95**, 016602 (2005).

[10] H. Najafov, I. Biaggio, V. Podzorov, M. F. Calhoun, and M. E. Gershenson, Phys. Rev. Lett. **96**, 056604 (2006).

[11] H. Najafov, B. Lyu, I. Biaggio, and V. Podzorov, Phys. Rev. B **77**, 125202 (2008).

[12] H. Najafov, B. Lyu, I. Biaggio, and V. Podzorov, Appl. Phys. Lett. **96**, 183302 (2010).

[13] I. Biaggio and P. Irkhin, Appl. Phys. Lett. **103**, 263301 (2013).

[14] P. Irkhin and I. Biaggio, Phys. Rev. Lett. **107**, 017402 (2011).

[15] O. D. Jurchescu, A. Meetsma, and T. T. M. Palstra, Acta Crystallogr., Sect. B **62**, 330 (2006).

[16] M. Rumi and J. W. Perry, Adv. Opt. Photonics **2**, 451 (2010).

[17] L. Ma, G. Galstyan, K. Zhang, C. Kloc, H. Sun, C. Soci, M. E. Michel-Beyerle, and G. G. Gurzadyan, J. Chem. Phys. **138**, 184508 (2013).

[18] L. Zhao, G. Yang, Z. Su, C. Qin, and S. Yang, Synth. Met. **156**, 1218 (2006).

[19] O.-K. Kim, K.-S. Lee, H. Y. Woo, K.-S. Kim, G. S. He, J. Swiatkiewicz, and P. N. Prasad, Chem. Mater. **12**, 284 (2000).

[20] M. Albota, D. Beljonne, J.-L. Brédas, J. E. Ehrlich, J.-Y. Fu, A. A. Heikal, S. E. Hess, T. Kogej, M. D. Levin, S. R. Marder *et al.*, Science **281**, 1653 (1998).

[21] A. Ryasnyanskiy and I. Biaggio, Phys. Rev. B **84**, 193203 (2011).

[22] Y. Chen, B. Lee, D. Fu, and V. Podzorov, Adv. Mater. **23**, 5370 (2011).

[23] N. Sai, M. L. Tiago, J. R. Chelikowsky, and F. A. Reboredo, Phys. Rev. B **77**, 161306 (2008).